Chapter 2

Puromycin Oligonucleotides Reveal Steric Restrictions For Ribosome Entry and Multiple Modes of Translation Inhibition

This chapter has previously appeared as: S.R. Starck and R.W. Roberts. Puromycin oligonucleotides reveal steric restrictions for ribosome entry and multiple modes of translation inhibition. *RNA* 8:890-903, 2002.

Abstract

Peptidyl transferase inhibitors have generally been studied using simple systems and remain largely unexamined in *in vitro* translation extracts. Here, we investigate the potency, product distribution, and mechanism of various puromycin-oligonucleotide conjugates (1 to 44 nucleotides with 3'-puromycin) in a reticulocyte lysate cell-free translation system. Surprisingly, the potency *decreases* as the chain length of the oligonucleotide is increased in this series, and only very short puromycin conjugates function efficiently ($IC_{50} < 50$ μM). This observation stands in contrast with work on isolated large ribosomal subunits which indicates that many of the puromycin-oligonucleotide conjugates we studied should have higher affinity for the peptidyl

transferase center than puromycin itself. Two $tRNA^{Ala}$-derived minihelices containing puromycin provide an exception to the size trend, and are the only constructs longer than four nucleotides with any appreciable potency ($IC_{50} = 40 - 56\ \mu M$). However, the puromycin minihelices inhibit translation by sequestering one or more soluble translation factors, and do not appear to participate in detectable peptide bond formation with the nascent chain. In contrast, puromycin and other short derivatives act in a factor-independent fashion at the peptidyl transferase center and readily become conjugated to the nascent protein chain. However, even for the short derivatives, much of the translation inhibition occurs *without* peptide bond formation between puromycin and the nascent chain, a revision of the classical model for puromycin function. This peptide bond-independent mode is likely a combination of multiple effects including inhibition of initiation and failure to properly recycle translation complexes that have reacted with puromycin.

2.1 Introduction

Puromycin has played an important role in our understanding of the ribosome and protein synthesis. It has been known for more than 40 years that the molecule is a universal protein synthesis inhibitor that acts as a structural analog of an aminoacyl-tRNA (aa-tRNA) (Figure 2.1) (1). Nathans went on to demonstrate that the ribosome mistakenly inserts puromycin in place of aminoacyl-tRNA resulting in truncated proteins containing the drug at their C-terminus (2). A later examination of this mechanism concluded that puromycin inhibits translation solely through C-terminal labeling of peptides and not through additional pathways (3). This classic model for puromycin supports only a single mode of action, covalent attachment to the nascent chain.

In vitro studies with the drug have largely utilized the 'fragment reaction,' in which peptidyl transferase activity of isolated 50S subunits is measured by the formation of

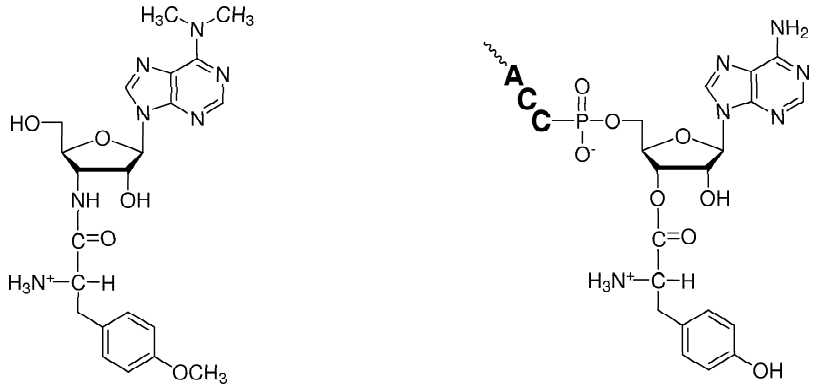

Figure 2.1: Puromycin versus aminoacyl-tRNA.

N-formyl-[^{35}S]Met-puromycin (f-Met-puromycin) from a fragment of *N*-formyl-Met-tRNA$_f^{Met}$ and puromycin (4). Much of what we know about the catalytic activity of the ribosome has been derived from this simple assay (5, 6). However, the reaction is conducted under conditions that are relatively non-physiological (30% ethanol, 400 mM K^+, and $0 - 4$ °C incubation temperature) and the effect of other critical components such as the template, small ribosomal subunit, and soluble translation factors cannot be measured, as they are absent. Thus, the potency of puromycin may not be accurately reflected by its activity under fragment reaction conditions.

To account for these shortcomings, some modifications have been made to more fully recapitulate the protein synthesis machinery. Addition of the small subunit and poly(U)-mRNA followed by P-site charging with *N*-acetyl-Phe-tRNA^{Phe} (Ac-Phe-tRNA^{Phe}) pushes the equilibrium towards subunit association, which allows peptidyl transferase to be carried out in the absence of alcohol (7). However, these adaptations still require salt-washed ribosomes, relatively high concentrations of NH_4Cl and $MgCl_2$ to promote subunit assembly in the absence of initiation factors (7), and fail to yield long polypeptide-puromycin complexes (>12-15 amino acids in the *E. coli* cell-free poly(A) system) (3). Thus even these modifications result in systems

that are biochemically removed from the complete translation apparatus. To date, the majority of studies with translation inhibitors have been conducted using either the classical fragment reaction or a version of the f-Met-tRNA·A-U-G·70S or Ac-Phe-tRNA·poly(U)·70S system (8, 9, 10, 11).

Interest in puromycin and puromycin conjugates has recently increased due to new methods for synthesizing molecular libraries (12, 13), photo-crosslinking reagents for the ribosome (8), peptidyl transferase inhibitors (11, 14), and *in vitro* synthesis of proteins containing specific labels or tags (15). Optimization of each of these processes requires that we understand how puromycin conjugates enter the ribosome in *cis* (when they are tethered to the mRNA in the decoding site) or in *trans* when these molecules enter the ribosome from solution. Considerable effort has recently gone into understanding the *cis* reaction to facilitate the synthesis of the mRNA-peptide fusions for mRNA-display selection experiments (16). Interestingly, the *trans* reaction between puromycin conjugates and the ribosome remains relatively uncharacterized in complete translation systems, and basic features, such as elongation factor dependence, remain unexplored. We were therefore curious to examine the ability of trans substrates to enter the ribosome and inhibit protein synthesis in a complete translation system. A deeper understanding of the trans reaction would be helpful in 1) synthesizing more efficient translation inhibitors, 2) creating better ribosome crosslinking reagents, and 3) using the ribosome to generate a protein tagged at its C-terminus.

Here, we have examined the effect of puromycin and puromycin-oligonucleotide conjugates on translation by constructing a series of oligonucleotides bearing puromycin at their 3'-end. We then assayed their ability to inhibit translation of rabbit globin mRNA in rabbit reticulocyte translation extracts. Our results differ markedly from previous work with isolated large subunits or whole ribosomes charged with artificial templates. The data provide new insights into the action of puromycin and identify constraints on the design of puromycin-based translation inhibitors that can

function in a physiologically relevant context.

2.2 Results and Discussion

2.2.1 Puromycin versus 30P

We began our experiments by comparing translation inhibition by two substrates, puromycin and 30**P** (p(dA)$_{27}$dCdC-**P**), a 30mer DNA oligonucleotide containing puromycin at the 3'-end. Previously, we had used 30**P** to tether puromycin to mRNAs for the synthesis of mRNA-peptide fusions (13). When attached to the mRNA template, 30**P** can act as an efficient peptide acceptor (13, 16). The design of 30**P** was based on previous work with isolated large subunits, which indicated that molecules containing a penultimate cytidine nucleotide adjacent to the aminoacyl nucleotide should be better acceptors than puromycin alone (reviewed in (?)). For example, 2'(3')-*O*-glycyladenosine (A-Gly) has little acceptor activity, whereas 1) addition of ribocytidine (C-A-Gly) gives a compound with similar activity to puromycin (17) and 2) CA-Phe has a lower K_m than A-Phe (18). Under fragment conditions, 4-thio-dT-C-puromycin has a lower K_m (10 μM) (8) than puromycin itself (K_m = 740 μM) (11). Taken together, these data support the notion that an oligonucleotide with dC-puromycin at its 3'-end should have higher acceptor activity than puromycin alone. However, preliminary experiments indicated that 30**P** showed little ability to inhibit translation or act as an acceptor when co-incubated with fusion templates (R.W.R., unpublished observation).

2.2.2 Potency of Puromycin and Puromycin Oligonucleotides

We developed an *in vitro* translation assay to quantify the potency of puromycin and other putative inhibitors such as 30**P**. In the assay, a translation reaction is performed for one hour using rabbit globin mRNA at ~60 nM (total template concentration; the

template is a mixture of α- and β-globin mRNAs) in rabbit reticulocyte lysate. Each reaction differs only in the amount of inhibitor that is added at the beginning of the reaction. We then assay the reactions by tricine-SDS PAGE (19), TCA precipitation, or other methods to determine the amount of globin translation product. This analysis results in a sigmoidal curve and we term the midpoint (the concentration of drug required to give a 50% decrease in globin synthesis relative to a no-inhibitor control) the IC_{50}.

IC_{50} determinations for puromycin and for 30**P** are shown in Figure 2.2. Several features can be seen in the gel analysis. First, globin synthesis decreases as the amount of puromycin is increased from 25 nM to 75 μM, resulting in an IC_{50} of 1.8 μM (Figure 2.2A,C). Our value agrees reasonably well with previous work showing an IC_{50} value of 2.8 μM in rabbit reticulocyte lysate (20). Our IC_{50} is $\sim$10- to 50-fold lower than the published K_d or K_m values for puromycin measured with mammalian ribosomes (21, 22). For example, Lorsch and Herschlag measured a K_m of $60-100$ μM for puromycin with rabbit reticulocyte ribosomes (22). Our lower apparent value is consistent with entry of puromycin at multiple sites in the protein chain, for example any one of the 144 or 148 codons (including stop) in rabbit α- or β-globin (23). The published K_m values thus provide support that we are measuring a composite of multiple mechanistic steps in our IC_{50} experiments.

A second feature observed for both inhibitors is the apparent lack of low molecular weight, truncated protein as the drug concentration is increased, even at the highest puromycin concentrations in this assay. As the puromycin concentration is increased, a gradual decrease in the amount of the globin band is seen with most of the remaining protein appearing as full-length globin. The fact that puromycin does not chase the protein into lower molecular weight species implies two possible mechanisms for its action: 1) that puromycin entry and peptide bond formation occur only at the termination step and not during elongation or 2) that puromycin entry results in fragments too small to be resolved by PAGE techniques (e.g., Met-puromycin). Analysis

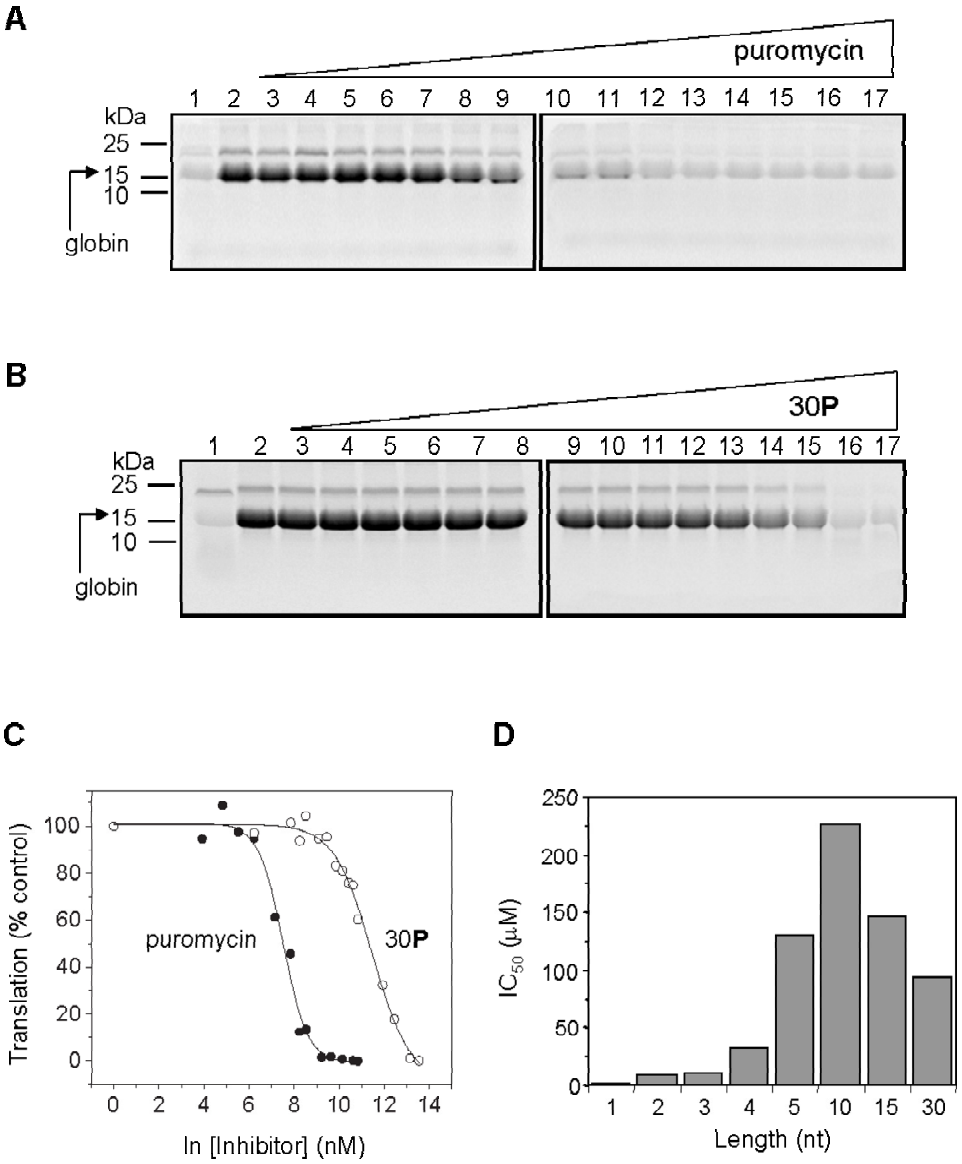

Figure 2.2: IC_{50} determinations for puromycin and 30**P**. (A) Translation of globin with puromycin: lane 1, no template; lane 2, globin alone; lanes 3 – 17, concentrations from 0.025 to 75 μM. (B) Translation of globin with 30**P**: lane 1, no template; lane 2, globin alone; lanes 3 – 16, 0.5 to 750 μM. (C) Percent of globin translation relative to a no-drug control for puromycin (•) and 30**P** (○). (D) Effect of chain length on IC_{50} values for puromycin and simple puromycin-oligonucleotide conjugates.

Inhibitor	IC_{50} (μM)
Linear Conjugates	
Puromycin (**P**)	1.8
r2**P** (prC-**P**)	9
2**P** (pdC-**P**)	10
3**P** (dCdC-**P**)	11
4**P** (dΛdCdC-**P**)	33
5**P** [$(d\Lambda)_2$dCdC-**P**]	130
10**P** [$(d\Lambda)_7$dCdC-**P**]	230
15**P** [$(d\Lambda)_{12}$dCdC-**P**]	150
30**P** [p$(d\Lambda)_{27}$dCdC-**P**]	94
tRNA Mimics	
RNA 12-**P**	56
Ala-minihelix-**P**	40
Oligonucleotides	
5Λ [$(d\Lambda)_2$dCdCdΛ]	>400
10Λ [$(d\Lambda)_7$dCdCdΛ]	1100
30Λ [$(d\Lambda)_{27}$dCdCdΛ]	>200
Ala-minihelix	83
Puromycin Derivatives	
biotin-puromycin	54
biotin-2**P** [biotin-dC-puromycin]	11
fluorescein-puromycin	120
N-trifluoroacetyl-puromycin	>250

Table 2.1: IC_{50} values for puromycin and puromycin oligonucleotide conjugates.

of the longer 30**P** oligonucleotide showed very weak inhibition with an IC_{50} ~100 μM, more than 50-fold weaker than puromycin (Figure 2.2B,C). In these experiments, the oligonucleotide phosphate concentration is significant compared to the divalent cation concentration in the translation extract (3 mM PO_4^- versus 0.5 mM Mg^{+2}). Indeed, the IC_{50} for an identical oligonucleotide lacking puromycin (30A; Table 2.1) was found to be >200 μM. Therefore, it appears that inhibition from 30**P** occurs from a combination of the action of puromycin as well as the high concentration of oligonucleotide in the translation reaction. This result indicates that the *trans* reaction is likely to be insignificant for mRNA-puromycin conjugates, as these are typically used at 100 nM to 1 μM concentrations (16). Comparing puromycin to 30**P** suggested that increasing the size of the puromycin conjugate decreases its potency. Further, addition of the -dAdCdC- sequence adjacent to puromycin did not enhance its efficacy as an inhibitor.

We therefore constructed a series of puromycin conjugates ranging from 1 to 44 nucleotides to examine these issues in more detail. Regarding size, we constructed a series of puromycin-DNA oligonucleotides with chain lengths of 2 (2**P**), 3 (3**P**), 4 (4**P**), 5 (5**P**), 10 (10**P**), and 15 (15**P**) nucleotides, in addition to puromycin and 30**P** (Table 2.1). Regarding compatibility with the acceptor site, we constructed a riboversion of 2**P** (prC-**P** = r2**P**) and two puromycin-RNA mimics of aa-tRNA. None of these molecules inhibited translation as effectively as puromycin. Generally, the IC_{50} values increase as the chain length is increased (Table 2.1 and Figure 2.2D). For example, addition of one nucleotide decreases the IC_{50} of puromycin by 5-fold (compare puromycin versus 2**P** or r2**P**; Table 2.1). The sugar moiety at the penultimate nucleotide makes little difference as the potency of r2**P** and 2**P** are nearly identical, in line with previous work on the Ac-Phe-tRNA·poly(U)·70S translation system (18). The IC_{50} values increase steadily from chains of one to five nucleotides. Above five nucleotides, puromycin conjugates give similar weak inhibition, with IC_{50} values ranging from 90 to 230 μM. The worst inhibitor is (dA)7dCdC-**P** (10**P**), which has an

IC_{50} value of 230 μM, similar to some oligonucleotides that lack puromycin entirely.

The data present a puzzle as to why the larger oligonucleotides are unable to act as effective inhibitors. The functional portion of all the molecules in the series is identical, the 3'-puromycin moiety. However, the potency of each ranges over more than 100-fold. Generally, the data support a model where size is a critical feature, suggesting that larger molecules are poor inhibitors due to difficulty entering the ribosome. Large molecules such as 30**P** are thus unable to enter the ribosome readily in a passive fashion. This hypothesis poses a problem since aa-tRNAs ranging from 75 to 90 nucleotides efficiently act as substrates in protein synthesis. However, aa-tRNAs enter the ribosome as a ternary complex with elongation factor (EF-Tu in bacteria and eEF1A in eukaryotes) and GTP.

We therefore tested whether puromycin conjugates that resembled aa-tRNAs would have greater efficacy as inhibitors. Previously, two alanylated $tRNA^{Ala}$-derived RNAs (denoted RNA 12 and Ala-minihelix) have been shown to bind bacterial EF-Tu with nanomolar affinity ($K_d = 4.5 - 29$ nM) (24). In addition, the Ala-minihelix has been shown to be as effective as Ala-$tRNA^{Ala}$ as an acceptor substrate in the bacterial fragment reaction (25). We constructed two puromycin-minihelix analogs of these sequences, RNA 12-**P** and Ala-minihelix-**P** (Figure 2.5), and examined their activity in our translation assay. Both RNA 12-**P** and Ala-minihelix-**P** are modest inhibitors of translation with IC_{50} values of 56 and 40 μM, respectively (Table 2.1). These values are more than 20-fold weaker than puromycin, but they are better than the longer oligonucleotide conjugates 10**P** and 30**P** by 2- to 4-fold, respectively. Interestingly, an Ala-minihelix lacking puromycin entirely (Ala-minihelix with 3'-adenosine), (Table 2.1) gave an IC_{50} of 83 μM, much better than any of the other simple oligonucleotides tested.

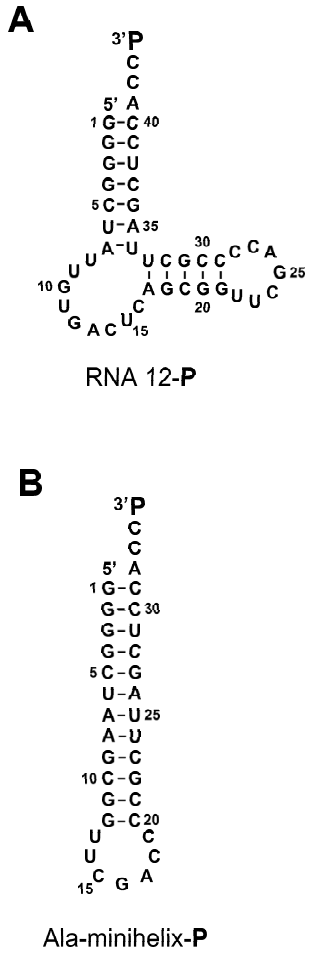

Figure 2.3: Secondary structure of tRNΛ mimics containing puromycin. Both (Λ) RNΛ 12-**P** and (B) Λla-minihelix-**P** were derived from *E. coli* $\text{tRN}\Lambda^{\Lambda\text{la}}$ (24).

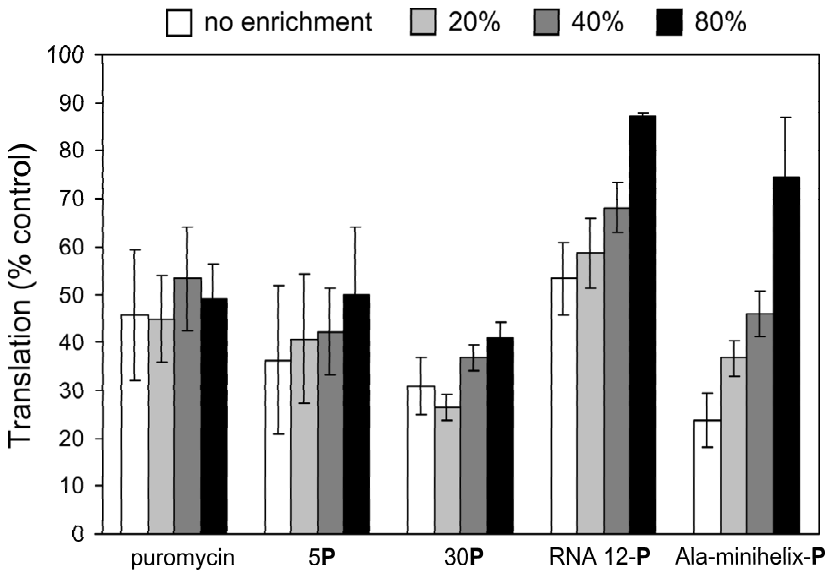

Figure 2.4: Effect of ribosome-depleted lysate on puromycin oligonucleotide-inhibited translation reactions. Addition of ribosome-depleted lysate does not change the amount of globin product significantly for reactions inhibited by puromycin, 5**P**, or 30**P**, but restores translation for both RNA 12-**P** and Ala-minihelix-**P**. The percent enrichment is given by the ratio of ribosome-depleted lysate to native lysate used in the reaction. The drug concentrations for each reaction are puromycin (3.8 μM), 5**P** (76 μM), 30**P** (56 μM), RNA 12-**P** (46 μM), and Ala-minihelix-**P** (46 μM). The values (mean $\pm$ S.E.) are the percent of translation compared to an untreated control.

2.2.3 Elongation Factor Dependence

The relatively strong inhibition by the puromycin-free Ala-minihelix implied that these compounds might inhibit translation by sequestering soluble translation factors. We generated a ribosome-depleted lysate (see Experimental Procedures) to test the role of soluble translation factors on the function of RNA 12-**P**, Ala-minihelix-**P**, and other puromycin conjugates. We added this ribosome-depleted fraction back to our normal translation reactions and assayed the translation of globin. If inhibitors act by sequestering soluble translation factors, then translation should be at least partially restored if more factors are added to the lysate. Inhibitors that work in a factor-independent fashion should be unaffected and inhibitors that require translation factors should become more potent.

Increasing amounts of ribosome-free lysate (relative to the amount of native lysate) had little or no effect on puromycin, 5**P**, or the 30**P** conjugates within experimental error (Figure 2.4). However, the added extract helped to recover translation in the presence of RNA 12-**P** and Ala-minihelix-**P** (Figure 2.4). At the highest level of enrichment (80%), translation was restored 34% and 50% in the presence of RNA 12-**P** and Ala-minihelix-**P**, respectively. This is a notable response since the extent of translation was fairly constant for puromycin, 5**P**, and 30**P** despite the increasing amounts of ribosome-depleted lysate. These results are consistent with a model where RNA 12-**P** and Ala-minihelix-**P** act by sequestering translation factors. These data also present the first clear evidence that puromycin and simple puromycin conjugates function in a translation factor-independent fashion in an intact translation system. The most likely candidate for interaction with the aminoacyl-tRNA^{Ala} mimics, RNA 12-**P** and Ala-minihelix-**P**, is elongation factor 1A (eEF1A). Both Ala-tRNA^{Ala}-derivatives, RNA 12 and Ala-minihelix, bind eEF1A with low nanomolar affinity ($K_d = 29$ and 84 nM, respectively). The three differences between these compounds and our analogs are 1) the amide linkage attaching the amino acid to the ribose, 2) the *O*-methyl tyrosine sidechain, and 3) the N6-dimethyl moiety. The sidechain likely has little effect

on elongation factor binding as many unnatural hydrophobic amino acids may be inserted into proteins in both bacteria (26) and in eukaryotes (27). The amide linkage and N6-dimethyl adenosine in our tRNA mimics may result in somewhat reduced affinity for the elongation factor (28).

We presently favor a model where RNA 12-**P** and Ala-minihelix-**P** act by sequestering eEF1A for two reasons: 1) inhibition occurs as the concentration of RNA-12-**P** or Ala-minihelix-**P** becomes comparable to the endogenous eEF1A concentration ($\sim$20 μM) and 2) this concentration is approximately 1000-fold higher than the reported K_ds for the Ala-RNA 12 and Ala-minihelix with eEF1A (29, 24). In this scenario, addition of minihelix titrates away the available pool of elongation factor until translation is entirely shutdown.

2.2.4 Product Distribution

The IC_{50} analysis using short tricine-SDS-PAGE gels revealed a lack of low molecular weight protein products for puromycin or any of the puromycin derivatives (Figure 2.2). These observations were somewhat unexpected, as it seemed puromycin should be able to enter the ribosome and become attached to the nascent chain at any time during elongation (2, 3). We were therefore curious 1) if puromycin entry occurred to a significant extent and 2) if our various conjugates differed in their ability to enter the ribosome.

We first analyzed the extent and distribution of products by constructing biotinylated versions of several puromycin conjugates. The four biotinylated puromycin conjugates tested include 1) biotin-puromycin, 2) biotin-dC-**P** (biotin-2**P**), 3) biotin-RNA 12-**P** (biotin-dT at position 11; see Figure 2.5) and 4) biotin-Ala-minihelix-**P** (biotin-dT at position 13; see Figure 2.5). We reasoned that any [^{35}S]Met-labeled peptide that became attached to these analogs, from one amino acid (initiator [^{35}S]Met) to full-length globin, could be easily detected by purification on streptavidin or monomeric avidin (see Experimental Procedures) followed by scintillation counting

or SDS-PAGE analysis.

Two of the derivatives, biotin-2**P** (Figure 2.5A,B) and biotin-RNA 12-**P** (data not shown), retain essentially the same IC_{50} as their parent compounds. However, these two biotin conjugates appear to act in decidedly different ways. Purification on streptavidin showed that [^{35}S]Met is not incorporated into biotin-RNA 12-**P**, indicating that this compound does not participate in peptide bond formation despite the fact that it can act as an inhibitor (data not shown). Our assay does not address whether the RNA 12-**P**·eEF1A·GTP ternary complex makes its way to the ribosome and is subsequently rejected during ribosomal substrate proofreading.

Biotin-2**P** is attached to significant amounts of nascent peptide (Figure 2.5C). This attachment occurs in a concentration dependent fashion, with a maximum at 35 μM of the conjugate. Even under optimal conditions, the amount of protein that is attached to puromycin is less than 40% of the total amount of protein made in the absence of drug (TCA precipitated globin) (Figure 2.5C). High-resolution tricine-SDS-PAGE analysis further supports these observations as lower molecular weight products are observed with puromycin and 5**P**, but not with RNA 12-**P** despite nearly complete inhibition of globin synthesis (data not shown).

The attachment of biotin-2**P** to the nascent peptide provided an excellent means to determine where puromycin entered the ribosome during elongation. After translation in the presence of biotin-2**P**, we purified the [^{35}S]Met-adducts using monomeric avidin-agarose (Pierce) (K_d, biotin = 10^{-8} M), released the products, and analyzed the fragments by tricine-SDS-PAGE. This gel identifies three discrete product bands (Figure 2.6). The highest molecular weight band is close to the full-length material (α-globin = 15.5 kDa and β-globin = 16 kDa), whereas the lower molecular weight bands appear to correspond to globin fragments of approximately 6 and 13 kDa (Figure 2.6). Biotin-2**P** concentrations up to 35 μM provide a concomitant increase in the amount of globin-biotin-2**P** complex (Figure 2.6A). Increasing concentrations also shift the product distributions of the three protein bands. Between 0.7 and 35 μM,

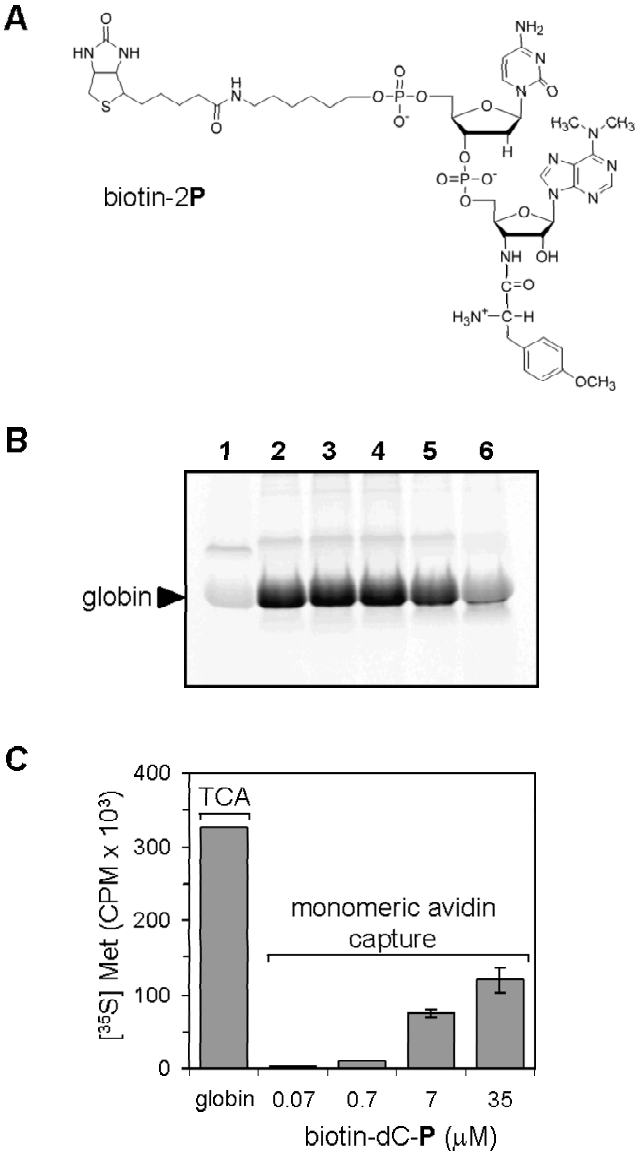

Figure 2.5: Translation inhibition and product formation for biotin-2**P**. (A) Structure of biotin-2**P**. (B) Translation inhibition with increasing amounts of biotin-2**P** assayed by tricine-SDS-PAGE: Lane 1, no globin and no biotin-2**P**; lane 2, globin alone; lane 3, 0.07 μM; lane 4, 0.7 μM; lane 5, 7.0 μM; and lane 6, 35 μM. (C) Isolation of [^{35}S]Met-labeled fragments linked to biotin-2**P** from reactions in (B) assayed by monoavidin capture.

the amount of the 6 and 13 kDa bands increases relative to the full-length product (Figure 2.6B). At 0.7 μM biotin-2**P**, the full-length product constitutes ~50% of the total counts, whereas at 35 μM, the 6, 13, and full-length bands have nearly equal intensity. The shift to lower molecular weight biotin-2**P**-globin fragments is fully consistent with increased ribosome entry at high drug concentrations.

It is important to note that quantification of protein-puromycin complexes in our assay is dependent on the presence of the [^{35}S]Met-label within the complex. However, initiator [^{35}S]Met is readily removed by a methionine aminopeptidase (MetAP) (30). Therefore, short peptide-puromycin complexes without the internal methionine (internal methionine is residue 32 in α-globin and 55 in β-globin) may not be detected in our radioassays. An exception to this is [^{35}S]Met-puromycin, which is not recognized by degradation machinery in reticulocyte lysate. Other than MetAP, no other degradation activity is expected to occur with our products (30).

Interestingly, neither biotin-puromycin (IC_{50} = 54 μM; Table 2.1) nor biotin-Ala-minihelix-**P** (data not shown) function efficiently as translation inhibitors, indicating that attachment of biotin interferes with their function. Addition of biotin to Ala-minihelix-**P** may block elongation factor binding and relieve eEF1A-mediated inhibition. The poor function for biotin-puromycin is more puzzling. Addition of the 5'-biotin-phosphate moiety to puromycin may interfere with A-site binding. In line with this observation, fluorescein-puromycin (5'-fluorescein-phosphate moiety) also functions very poorly as a translation inhibitor, with an IC_{50} of 120 μM (Table 2.1). Whatever the origin, the poor potency of 5'-biotin-puromycin and 5'-fluorescein-puromycin provide a clear design constraint, namely that fluorescent and affinity tag labels should be appended to 5'-end of a dC-**P** or rC-**P** dinucleotide to maximize their incorporation into nascent chains.

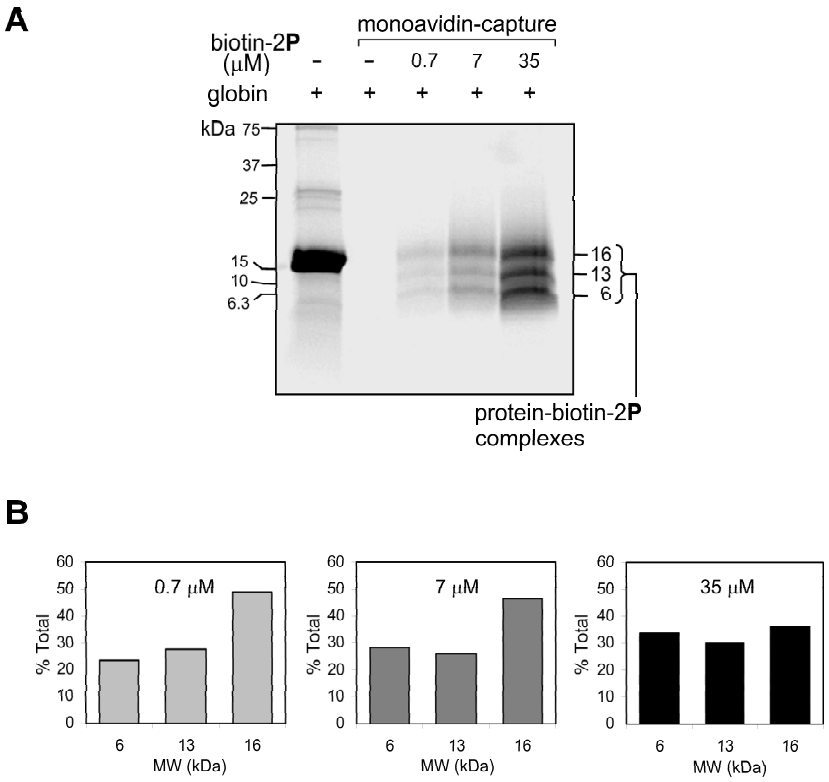

Figure 2.6: Analysis and quantitation of globin fragments attached to biotin-2**P** after translation. (A) High-resolution tricine-SDS-PAGE analysis of fragments bound to biotin-2**P**. Fragments were captured after translation with monomeric avidin, released and analyzed (see Experimental Procedures). Three distinct globin products are seen with approximate molecular weights of 6, 13, and 16 kDa. Increasing concentrations of drug results in an increasing amount of biotin-2**P**-bound product. (B) Ratio of [^{35}S]Met counts in 6, 13 and 16 kDa bands. As the biotin-2**P** concentration is increased, the product distribution shifts toward the lower molecular weight fragments. Fragments ~32 (α-globin) and ~55 amino acids (β-globin) may not be seen since the [^{35}S]Met-label is not present (see Conclusions).

2.2.5 Puromycin Entry At Ribosome Pause Sites

The monomeric avidin capture experiments demonstrate that three [^{35}S]Met-puromycin-containing protein fragments are generated using biotin-2**P**. These data indicate that puromycin entry occurs preferentially at relatively few positions. Mechanistically, these preferences could occur if 1) ribosomes were paused at these sites or 2) these positions were hyper-reactive to puromycin. Our results cannot distinguish these two models, but there is presently no data to indicate that certain codons are hyper-reactive to puromycin.

In contrast, there is support for pausing at discrete locations within the message (31). Wolin and Walter found that eukaryotic ribosomes (wheat or rabbit) pause at two internal positions (on glycine residues 77 and 159) and at the start and terminus of the preprolactin mRNA (31). In our sequences, β-globin contains glycines at positions 47 and 120, and α-globin contains glycine at position 52 and 60. These glycines could be the source of pausing in our templates. It is not clear why pausing would occur at these positions as opposed to other glycines in the open reading frames, in line with Wolin's and Walter's observations. We note that in β-globin mRNA Gly47 and Gly120 occur in the same sequence context, directly after a phenylalanine residue. Our biotin-capture assay may therefore provide a technically straightforward way to assay discrete ribosome pause sites.

2.2.6 Preincubation and Carboxypeptidase Analysis

Puromycin added at the start of the reaction (at concentrations several-fold higher than the ribosome concentration) may inhibit the formation of an initiation complex by binding in the A- or P-sites and perturb the assembly of an initiation complex. Formation of Met-puromycin or short peptide-puromycin fragments (not bearing the internal [^{35}S]Met) would also be an explanation for the complete loss of translation at high puromycin concentrations. Both of these predictions could not be resolved simply

by SDS-PAGE analysis as carried out in Figure 2.2. Instead, preincubation of lysate reactions with template prior to addition of puromycin could indicate whether A- or P-site binding or some other binding mode predominates. Further, the examination of puromycin potency with template preincubation could clarify whether the production of Met-puromycin or short protein-puromycin complexes is the principal action of puromycin.

We therefore preincubated our translation reactions for 30 seconds, 1 minute, or 5 minutes prior to addition of biotin-2**P**, and determined the IC_{50} and product distributions. Reaction products were purified on streptavidin-agarose and quantitated by scintillation counting (see Experimental Procedures). Reactions with biotin-2**P** concentrations <35 μM for all preincubation times indicate that the amount of both free and bound globin remains nearly unchanged (compare no preincubation with 1 min preincubation, Figure 2.7A,B). We observe nearly equivalent IC_{50} values for biotin-2**P** whether biotin-2**P** is added at the beginning of translation (IC_{50} = 11 μM) or after translation has had time to commence on all templates (IC_{50} = 16 μM). This suggests that inhibition results from biotin-2**P** occupation of regions not sensitive to initiation complex formation and/or a mechanism that inhibits ribosome recycling. The observation that maximum complex formation occurs at ~35 μM concentration is qualitatively similar to the concentration optimum of 20 μM for crosslinking, obtained with 4-thioT-rC-puromycin on bacterial ribosomes (8).

At very high drug concentrations (e.g., 140 μM), one and five minute preincubations result in a 4- to 5-fold increase in the amount of globin attached to biotin-2**P**, respectively (Figure 2.7B, 5 min preincubation not shown). The increase in biotin-2**P**-globin products likely represents the fraction of templates that initiate translation in the first 1 to 5 minutes. The large excess of biotin-2**P** present then results in attachment of the drug to the majority of the nascent chains. Further rounds of translation are possibly arrested by biotin-2**P** blocking initiation, inhibition of ribosome recycling, or inactivation of 60S subunits from obstruction of the exit tunnel

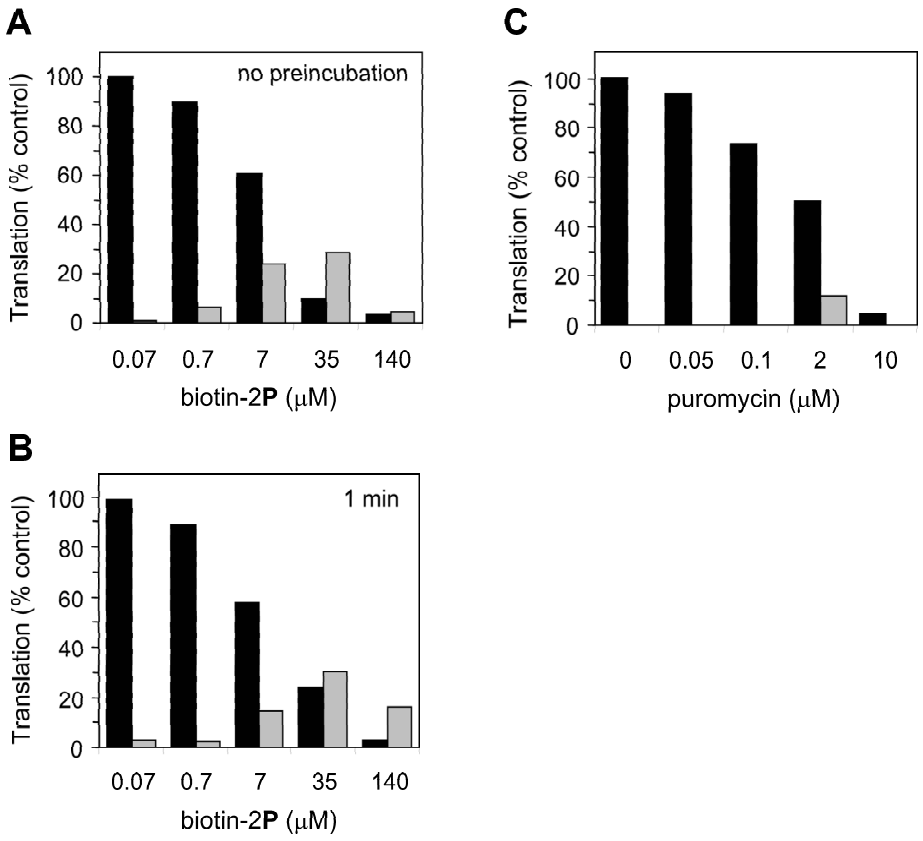

Figure 2.7: Analysis of puromycin-conjugated globin 1) by streptavidin-capture of biotin-2**P** and 2) carboxypeptidase Y treatment. Translation reactions were preincubated at 30 °C for (A) 0 min and (B) 1 min prior to addition of biotin-2**P**. The inhibition profiles for all cases, given by the globin translation (black bar), are the same within experimental error. The amount of globin fragment attached to biotin-2**P** (grey bar) increases only for the high concentration sample (140 μM). (C) Globin fragments containing a C-terminal puromycin are carboxypeptidase Y-resistant. Graph of the total globin made (black bar) and carboxypeptidase Y-resistant globin (grey bar) as a function of puromycin concentrations. The synthesis of puromycin-reacted globin products show an optimum at $\sim$2 μM of puromycin.

with peptide-puromycin- oligonucleotide conjugates.

Our data do not support the notion that the majority of inhibition results from production of Met-puromycin, since preincubation has little effect on the amount of [^{35}S]Met material isolated. Additionally, no Met-puromycin is detected in lysate reactions using the cation-exchange TLC assay developed previously to study the formation of Met-puromycin (22) (data not shown). Finally, we observe no significant shift in the IC_{50} value with preincubation, as would be expected if the majority of puromycin entry occurred in the first few codons. Overall, these analyses are consistent with the conclusion that short peptide-puromycin conjugates are not produced in significant quantity in our reactions.

Another method to identify puromycin-labeled protein is carboxypeptidase analysis, which was originally used to demonstrate puromycin attachment to nascent protein chains (2). After carboxypeptidase Y (CPY) digestion of puromycin-treated translation reactions, very little CPY-resistant protein was detected (Figure 2.7C). Indeed, CPY-resistant protein is detected above the no-drug control only when the drug concentration approaches the IC_{50} value of the compound (2 μM for puromycin). This data confirms that puromycin is able to enter the ribosome and become attached to the nascent protein. However, the amount of CPY-resistant product (12% of the no-drug control) is minimal (Figure 2.7C) and resembles the fraction of globin that becomes attached to biotin-2**P** (Figure 2.7A,B). These experiments further support the multiple-mode hypothesis for puromycin action 1) bonding to the C-terminus of a nascent protein and 2) through a mechanism that does not result in covalent attachment to protein.

2.2.7 Role of the Free Amine

Puromycin is produced by *Streptomyces alboniger* despite its sensitivity to the drug (32). *S. alboniger* inhibits the lethality of the drug by *N*-acetylation of the reactive amino group, thereby eliminating its acceptor activity in protein synthesis (33). We

constructed an *N*-acetylated version of puromycin (*N*-trifluoroacetyl-puromycin) and measured the IC_{50} value to see if this modification eliminated activity of the drug. For example, if the acetylated version could bind the P-site, it might inhibit translation at high concentrations. Our results demonstrate that the *N*-acetylated puromycin molecule is virtually inactive in blocking protein synthesis in reticulocyte lysate (IC_{50} >250 μM) (Table 2.1). The free amine group on puromycin is thus essential for both the peptide-bond dependent and peptide bond-independent action of puromycin.

2.2.8 Revised Model for Puromycin Action: Multiple Modes of Inhibition

Broadly, we observe two modes of puromycin action: 1) a covalent attachment mode and 2) a non-covalent mode. The covalent mode represents the classical activity of puromycin, peptide bonding to the C-terminus of the nascent chain (2, 3). This model implies that the number of moles of globin made in the absence of drug should equal the total moles of free globin plus puromycin-bound globin when the drug is present. Our observations differ from this prediction (Figures 2.5 – 2.8). The non-covalent mode is evident from the summation of free [^{35}S]Met-globin and [^{35}S]Met-globin bound to biotin-2**P**, which does not nearly equal the amount of protein synthesis in a no-drug control at drug concentrations >35 μM (Figure 2.8). The non-covalent mode can be broken down into a combination of multiple effects including 1) inhibition of ribosome recycling, 2) inhibition of an initiation or translation-competent complex, and 3) sequestration of soluble factors (tRNA mimics only) (Figure 2.9). Inhibition of ribosome recycling could result from a combination of events including 1) failure of puromycin-reacted ribosomes to be recognized by the normal recycling apparatus or 2) inactivation of the large subunit from congestion in the exit tunnel/P-site with a peptide-puromycin-oligonucleotide conjugate, preventing further rounds of translation.

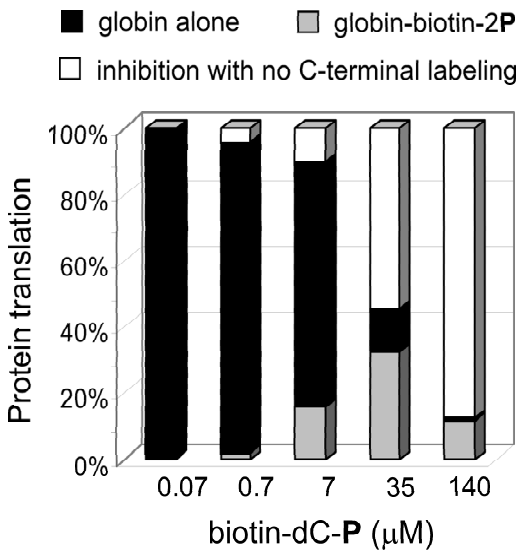

Figure 2.8: Quantitation of free globin, biotin-2**P** conjugated globin, and amount of protein synthesis inhibition. Plot of the amount of globin (black bar), biotin-2**P** conjugated globin (grey bar), and the amount of translation inhibition (white bar) as a function of biotin-2**P** concentration. The free globin protein product falls steadily above 7 μM biotin-2**P**, whereas the amount of puromycin-reacted product shows an optimum around 35 μM of the drug. The sum of the two globin fractions does not equal 100% above 7 μM of biotin-2**P**.

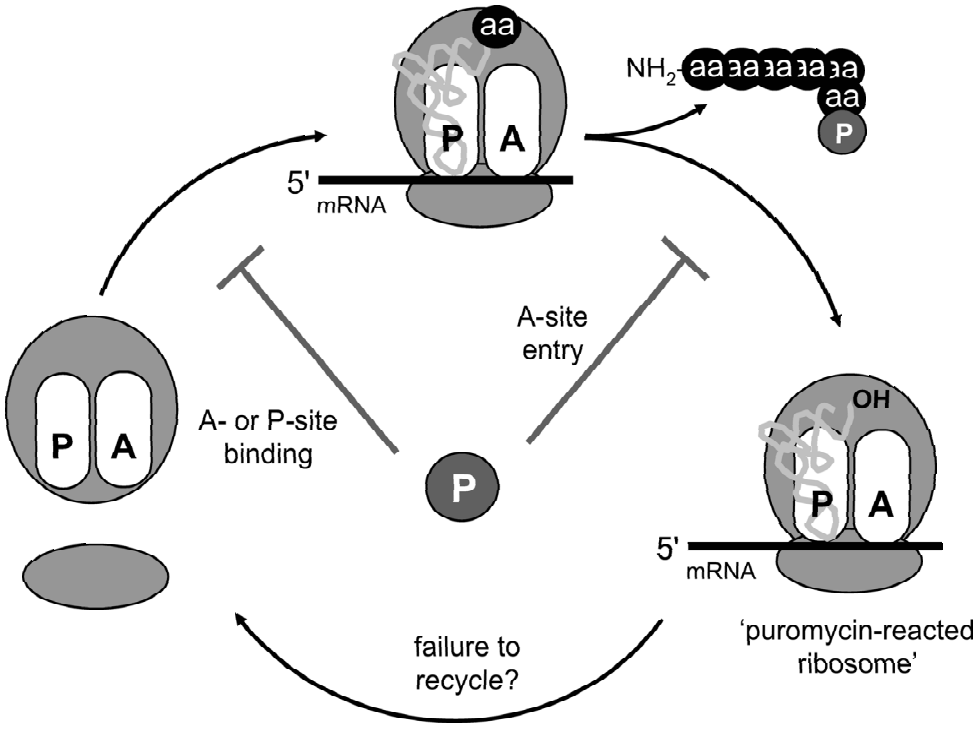

Figure 2.9: Revised model for the action of puromycin-oligonucleotides. Puromycin-oligonucleotides may function in a peptide bond-dependent mode, attaching to the nascent peptide to give puromycin-bound protein products. These same puromycin-oligonucleotides may also act in a peptide bond-independent fashion that represents a composite of different mechanisms including 1) inhibition of translation initiation by binding in the A- or P-sites, 2) inhibition of ribosome recycling, and 3) sequestering soluble translation factors (tRNA mimics only).

2.2.9 Size, Rather than Affinity, Determines Potency of Puromycin Conjugates

We observe that the efficacy of our puromycin conjugates depends primarily on their size, rather than their affinity for the ribosome. Overall, larger derivatives show weaker potency as inhibitors, with some functioning only a few-fold better than oligonucleotides lacking puromycin. This finding is in stark contrast to studies on isolated bacterial 50S subunits. For example, the overall affinity of 2'-(3')-*O*-aminoacyl derivatives of CA is considerably greater than that of the analogous adenosine derivatives. Previous work demonstrates that 4-thio-dT-rC-**P** has a K_m value of 10 μM with bacterial ribosomes (8) as compared with a K_m of 740 μM for puromycin itself (11) under the fragment assay conditions. However, our data show that the 2**P** conjugates (prC-**P** and pdC-**P**) are five times less potent than puromycin (Table 2.1). Certainly this result is not intuitive since the dC (analogous to the penultimate C in tRNA) is expected to Watson-Crick base pair in the A-loop (8, 14) and is therefore expected to be a better acceptor than puromycin alone. The presence of yet another base should contribute to the free energy of stabilization through base stacking in the A-loop (14). Our results demonstrate that addition of another dC to make dCdC-**P** (3**P**) decreases rather than improves the potency of the inhibitor (Table 2.1). Thus, the efficacy of our puromycin conjugates does not show correlation with expected A-site affinity.

The present literature would also predict that adding nucleotides to the 5'-end of our conjugates would have no effect on acceptor activity. This prediction also differs from our observations. For example, CCA-Phe and CACCA-Phe bind equivalently to bacterial ribosomes (34, 35). In contrast, we observe that adding nucleotides beyond dCdC-**P** diminishes the IC_{50} for the conjugates significantly (Table 2.1). For example, addition of dA to give dAdCdC-**P** (4**P**) results in a 3-fold loss of activity relative to 3**P** and a compound that is 18-fold worse than puromycin (Table 2.1).

Our results lead us to conclude that entry into the A-site, rather than affinity

for the ribosome, is the primary determinant of activity in the series of molecules we have investigated. Puromycin-conjugate function apparently is determined by how efficiently they are able to enter or leak into the ribosome. The path puromycin conjugates must traverse to act as substrates appears to allow only relatively small molecules to enter in a factor-independent fashion.

2.3 Conclusions

Our experiments demonstrate that puromycin and its derivatives may inhibit translation in multiple ways. First, small puromycin derivatives can enter the peptidyl transferase center and become attached to the nascent protein chain in a factor-independent fashion. Derivatives that resemble tRNA can inhibit translation by sequestering soluble factors, likely eEF1A. Puromycin attachment occurs predominantly at discrete locations within the template and near the end of the open reading frame. Second, our data indicate that puromycin can function in a peptide bond-independent mode. This inhibition is likely due to a combination of puromycin binding that blocks initiation, failure of ribosomes to recycle properly, or some other non-productive mode.

Our results have both practical and broader implications. First, these data should aid in the design and testing of efficient peptidyl transferase inhibitors as well as the synthesis of protein-puromycin conjugates *in vitro*. Entry of biotin-2**P** at discrete locations along the message may provide a fast, simple means to assay translational pausing within a particular template. Biotin-2**P** may also find use in cellular labeling experiments, to tag portions of cells that are actively synthesizing proteins for fluorescence *in situ* detection (B. Hay, personal communication). Finally, our data demonstrate striking differences in peptidyl transferase inhibitor potency when minimal translation systems are compared to those that are physiologically more complete.

2.4 Experimental Procedures

2.4.1 Reagents

Puromycin hydrochloride and d-biotin were obtained from Sigma Chemical Co. (St. Louis, MO). Rabbit reticulocyte Red Nova lysate was purchased from Novagen (Madison, WI). Rabbit globin mRNA was obtained from Life Technologies Gibco BRL (Rockville, MD) and Novagen (Madison, WI). L-[^{35}S]methionine ([^{35}S]Met) (1175 Ci/mmol) was obtained from NEN Life Science Products (Boston, MA). Carboxypeptidase Y and Immunopure immobilized monomeric avidin and streptavidin-agarose were from Pierce (Rockford, IL). GF/A glass microfiber filters were from Whatman. Polygram IONEX-25 SA-Na cation exchange TLC plates were purchased from Alltech (Deerfield, IL). Microcon YM-3 (3,000 MW cutoff) centrifugal filter columns were obtained from Millipore (Bedford, MA).

2.4.2 Oligonucleotides

RNA and DNA oligonucleotides and puromycin-oligonucleotide conjugates were synthesized using standard phosphoramidite chemistry at the California Institute of Technology oligonucleotide synthesis facility. Puromycin-CPG was obtained from Glen Research (Sterling, VA). Oligonucleotides were synthesized with the 5'-trityl intact, desalted via OPC cartridge chromatography (Glen Research) (DNA oligonucleotides only), cleaved, and evaporated to dryness. 5'-Biotin phosphoramidite and biotin-dT (Glen Research) were used to make the biotin-puromycin conjugates. The dried samples were resuspended and desalted by sephadex chromatography. The puromycin-oligonucleotides pC-**P** (r2**P**), pdC-**P** (2**P**), biotin-dC-**P** (biotin-2**P**), dCdC-**P** (3**P**), dAdCdC-**P** (4**P**), and $(dA)_2$dCdC-**P** (5**P**) were desalted on Sephadex G-10 (Sigma), all others were desalted on Sephadex G-25 (Sigma). Urea PAGE analysis confirmed that each oligonucleotide was a single species. Short oligonucleotides display anomalously slow electrophoretic mobility due to the positively charged puromycin.

The RNA r2**P** was deprotected with 1 M tetrabutylammonium fluoride (TBAF) in tetrahydrofuran (THF) (Aldrich) according to the method described in (36) and purified to homogeneity using HPLC with a Dionex DNAPac PA-100 semi-preparative column (9 x 250 mm) with buffer A (10 mM NH_4OAc (pH 5.5) + 10% acetonitrile) and buffer B (200 mM NH_4OAc (pH 5.5) + 10% acetonitrile); a linear gradient of 90% buffer B in 20 min was used with a flow rate of 1.5 mL/min. The RNAs Ala-minihelix-**P** and RNA 12-**P** (including biotinylated-derivatives) were deprotected with *N*-methylpyrrolidinone (Aldrich), anhydrous triethylamine (Aldrich), and anhydrous triethylamine-hydrogen fluoride (Aldrich) as described in (37) and purified by 20% denaturing PAGE. Puromycin and puromycin-oligonucleotides concentrations were determined with the following extinction coefficients ($M^{-1}cm^{-1}$) at 260 nm: puromycin (ϵ = 11,790), r2**P** (ϵ = 18,920), d2**P** (ϵ = 19,100), 3**P** (ϵ = 26,210), 4**P** (ϵ = 41,200), 5**P** (ϵ = 52,200), 10**P** (ϵ = 112,200), 15**P** (ϵ = 172,200), 30**P** (ϵ = 352,200), Ala-minihelix-**P** (ϵ = 324,100), and RNA 12-**P** (ϵ = 409,700).

2.4.3 IC_{50} Determination

Translation reactions containing [^{35}S]Met were mixed in batch on ice and added in aliquots to microcentrifuge tubes containing an appropriate amount of puromycin, puromycin-conjugate, or oligonucleotide dried in vacuo. Typically, a 20 μl translation mixture consisted of 0.8 μL of 2.5 M KCl, 0.4 μL of 25 mM MgOAc, 1.6 μL of 12.5X translation mixture without methionine, (25 mM dithiothreitol (DTT), 250 mM HEPES (pH 7.6), 100 mM creatine phosphate, and 312.5 μM of 19 amino acids, except methionine) (Novagen), 3.6 μL of nuclease-free water, 0.6 μL (6.1 μCi) of [^{35}S]Met (1175 Ci/mmol), 8 μL of Red Nova nuclease-treated lysate (Novagen), and 5 μL of 0.05 μg/μL globin mRNA (Gibco). Inhibitor, lysate preparation (including all components except template), and globin mRNA were mixed simultaneously and incubated at 30 °C for 60 min. For some assays (e.g., detection of small protein fragments and biotin-capture experiments, see below) the amount of [^{35}S]Met (1175

Ci/mmol) in a 20 μL reaction was increased to 4.2 μL (43 μCi) and no nuclease-free water was added. Then 2 μL of each reaction was combined with 8 μL of tricine loading buffer (80 mM Tris-Cl (pH 6.8), 200 mM DTT, 24% (v/v) glycerol, 8% sodium dodecyl sulfate (SDS), and 0.02% (w/v) Coomassie blue G-250), heated to 90 °C for 5 min, and applied entirely to a 4% stacking portion of a 16% tricine-SDS-polyacrylamide gel containing 20% (v/v) glycerol (19) (30 mA for 1h, 30 min). Gels were fixed in 10% acetic acid (v/v) and 50% (v/v) methanol, dried, exposed overnight on a PhosphorImager screen, and analyzed using a Storm PhosphorImager (Molecular Dynamics). IC_{50} determination for N-trifluoroacetyl-puromycin was conducted as above except the inhibitor was initially dissolved in dimethyl sulfoxide (DMSO) and the final DMSO concentration in each translation reaction was 5% (v/v). Fluorescein-puromycin (dissolved in 3 mM Na_2CO_3/$NaHCO_3$) was added in aliquots to lysate preparations as described above, except 1 μL of 0.25 μg/μL globin mRNA (Novagen) and additional nuclease-treated water was used in each 20 μL reaction.

2.4.4 Lysate Enrichment Assay

Ribosome-depleted rabbit reticulocyte lysate was prepared by ultracentrifugation of 80 μL/rotor tube of Red Nova lysate at 95,000 RPM for 30 min at 4 °C in a Beckman Airfuge Ultracentrifuge (A-100 rotor with 5 x 20 mm tubes). Lysate preparation (15 μL) and template (5 μL of 0.05 μg/μL globin mRNA) were mixed simultaneously in microcentrifuge tubes containing puromycin and puromycin-oligonucleotides dried *in vacuo*. A typical 20 μL reaction mixture contained the following: 0.8 μL of 2.5 M KCl, 0.4 μL of 25 mM MgOAc, 1.6 μL of 12.5X Translation Mixture without methionine, 0.6 μL of [^{35}S]Met (1175 Ci/mmol), 6.8 μL of Red Nova nuclease-treated lysate plus 0, 1.4, 2.7, or 5.3 μL of ribosome-depleted lysate and 5.3, 4.0, 2.6, or 0 μL of nuclease-free water for 0, 20, 40, and $\sim$ 80% enrichment (relative to the amount of native lysate/reaction), respectively. The samples were analyzed as described above for IC_{50} determination.

2.4.5 TLC Assay for Detection of Met-puromycin

The standard assay as described for IC_{50} determination was carried out except 45 μCi of [^{35}S]Met was used in each translation mix. After incubation, aliquots (1 μL) were spotted onto Polygram IONEX-25 SA-Na cation exchange TLC plates (9 X 11 cm) and developed in 2 M ammonium acetate (pH 5.2) plus 10% acetonitrile as described in (22). The plates were dried, exposed overnight on a PhosphorImager screen, and analyzed on a Storm PhosphoImager. The position of 4**P** was determined through UV-shadow of the sample TLC plate and the position of [^{35}S]Met-tRNA is assumed from an equivalent experiment described in (22).

2.4.6 Monomeric Avidin- and Streptavidin-capture of Biotinylated Puromycin Conjugates

Biotin-RNA 12-**P** (biotin-dT at position 11 in Figure 2.4), biotin-Ala-minihelix-**P** (biotin-dT at position 13 in Figure 2.4), or biotin-2**P** were evaporated to dryness in microcentrifuge tubes followed by simultaneous addition of 15 μL of lysate preparation (components are the same as for IC_{50} determination, but with 43 μCi of [^{35}S]Met/reaction) and 5 μL of 0.05 μg/μL globin mRNA. The reactions were incubated at 30 °C for 60 minutes. For the monoavidin-agarose experiments [50% slurry (v/v)], the high affinity biotin-binding sites were blocked with a solution of 2 mM D-biotin in phosphate buffered saline (PBS) (137 mM NaCl, 2.7 mM KCl, 4.3 mM $Na_2HPO_4 \cdot 7H_2O$, 1.4 mM KH_2PO_4, and 0.1% Triton X-100) followed by removal of D-biotin from low affinity biotin-binding sites using 0.1 M glycine (pH 2.8) (0.1% Triton X-100) according to manufacturer instructions. Typically, 0.6 mL of the monoavidin-agarose 50% slurry (v/v) was pre-blocked as described above, washed 3 times with PBS, and resuspended in 1 mL of PBS. Aliquots of this suspension (125 μL) were combined with 7.5 μL of the reaction lysate mixture and 0.575 mL of PBS for each reaction. The samples were rotated at 4 °C for 1.5 h and then washed with PBS un-

til the CPM of [^{35}S]Met were < 1000 in the wash. The biotin-immobilized molecules were eluted with 2 mM D-biotin in PBS and concentrated to < 20 μL in YM-3 Microcon centrifugal filters. Tricine loading buffer (20 μL) was added to the concentrated samples and applied entirely to a 4/16% tricine-SDS-polyacrylamide gel (30 mA, 5 h). For streptavidin-capture experiments, 0.6 mL of streptavidin-agarose [50% slurry (v/v)] was washed 3 times with PBS and resuspended in 1 mL of PBS. To 100 μL of this suspension, 3 μL of the reaction lysate and 0.4 mL of PBS were added. The samples were rotated at 4 °C for 3 h and washed with PBS until the CPM of [^{35}S]Met were <500 in the wash. The amount of immobilized [^{35}S]Met-protein-puromycin conjugate was determined by scintillation counting of the streptavidin-agarose beads. An incorporation assay was used to determine the amount of globin synthesized (no inhibitor control) in an equivalent volume of lysate. After incubation, 3 μL of the lysate reaction was mixed with 150 μL of 1 N NaOH/2% H_2O_2 and incubated at 37 °C for 10 min to hydrolyze the charged tRNAs. Then 1.35 mL of 25% trichloroacetic acid (TCA)/2% casamino acids was added to the samples, vortexed, and put on ice for 10 min. The samples were filtered on GF/A filters (pre-soaked in 5% TCA), washed 3 times with 4.5 mL of cold 5% TCA, dried under high heat, and scintillation counted to determine the amount of [^{35}S]Met-globin.

2.4.7 Preincubation Assay with Biotin-2P

Lysate preparation (15 μL, prepared as described above with 43 μCi [^{35}S]Met/reaction) and globin mRNA (1 μL of 0.25 μg/μL, Novagen) were preincubated at 30 °C for 0, 1, or 5 min. After addition of biotin-2**P** (3 μL aliquots) and nuclease-free water (1 μL), the reactions were incubated at 30 °C for an additional 60 min. Analysis of the translation reactions via streptavidin-agarose capture was carried out exactly as described above.

2.4.8 Carboxypeptidase Y Assay

Translation reactions were prepared and treated as described for IC_{50} determination (43 μCi [^{35}S]Met/reaction). A portion of each lysate reaction (2.5 μL) was resuspended in 23 μL of 0.1 M sodium acetate (pH 5.0) and carboxypeptidase Y [15 μL of 1 mg/mL in 0.05 M sodium citrate (pH 5.3)] was added followed by incubation at 37 °C for 14 h. After incubation, the samples were concentrated to <5 μL and 10 μL of tricine loading buffer was added. The samples were analyzed using 4/16% tricine-SDS-PAGE as described above.

Acknowledgements

We thank Ms. Jie Xu for synthesis of *N*-trifluoroacetyl-puromycin, and Terry T. Takahashi for comments on this manuscript. This work was supported by NIH Grant R01 GM60416 to R.W.R. and by NIH training grant GM 07616 (S.R.S.).

References

[1] M.B. Yarmolinsky and G. de la Haba. Inhibition by puromycin of amino acid incorporation into protein. *Proc. Natl. Acad. Sci. U.S.A.*, 45:1721–1729, 1959.

[2] D. Nathans. Puromycin inhibition of protein synthesis: incorporation of puromycin into peptide chains. *Proc. Natl. Acad. Sci. U.S.A.*, 51:585–592, 1964.

[3] J.D. Smith, R.R. Traut, G.M. Blackburn, and R.E. Monro. Action of puromycin in polyadenylic acid-directed polylysine synthesis. *J. Mol. Biol.*, 13:617–628, 1965.

[4] RE. Monro and KA. Marcker. Ribosome-catalysed reaction of puromycin with a formylmethionine-containing oligonucleotide. *J. Mol. Biol.*, 25:347–350, 1967.

[5] HF. Noller, V. Hoffarth, and Zimniak L. Unusual resistance of peptidyl transferase to protein extraction procedures. *Science*, 256:1416–1419, 1992.

[6] R.R. Samaha, R. Green, and H.F. Noller. A base pair between tRNA and 23S rRNA in the peptidyl transferase centre of the ribosome. *Nature*, 377:309–314, 1995.

[7] S. Chládek, D. Ringer, and J. Žemlička. L-phenylalanine esters of open-chain analog of adenosine as substrates for ribosomal peptidyl transferase. *Biochemistry*, 12:5135–5138, 1973.

[8] R. Green, C. Switzer, and HF. Noller. Ribosome-catalyzed peptide-bond formation with an A-site substrate covalently linked to the 23S ribosomal RNA. *Science*, 280:286–289, 1998.

[9] M. Michelinaki, P. Namos, C. Coutsogeorgopoulos, and D.L. Kalpaxis. Aminoacyl and peptidyl analogs of chloramphenicol as slow binding inhibitors of ribosomal peptidyltransferase: A new approach for evaluating their potency. *Mol. Pharm.*, 51:139–146, 1996.

[10] O.W. Odom and B. Hardesty. Use of 50S-binding antibiotics to characterize the ribosomal site to which peptidyl-tRNA is bound. *J. Biol. Chem.*, 267:19117–19122, 1992.

[11] M. Welch, J. Chastang, and M. Yarus. An inhibitor of ribosomal peptidyl transferase using transition-state analogy. *Biochemistry*, 34:385–390, 1995.

[12] N. Nemoto, E. Miyamoto-Sato, Y. Husimi, and H. Yanagawa. *In vitro* virus: Bonding of mRNA bearing puromycin at the 3'-terminal end to the C-terminal end of its encoded protein on the ribosome *in vitro*. *FEBS Lett.*, 414:405–408, 1997.

[13] R.W. Roberts and J.W. Szostak. RNA-peptide fusions for the *in vitro* selection of peptides and proteins. *Proc. Natl. Acad. Sci. U.S.A.*, 94:12297–12302, 1997.

[14] P. Nissen, J. Hansen, N. Ban, PB. Moore, and Steitz TA. The structural basis of ribosome activity in peptide bond synthesis. *Science*, 289:920–930, 2000.

[15] E. Miyamoto-Sato, N. Nemoto, K. Kobayashi, and H. Yanagawa. Specific bonding of puromycin to full-length protein at the C-terminus. *Nucleic Acids Res.*, 28:1176–1182, 2000.

[16] R. Liu, J. Barrick, J.W. Szostak, and R.W. Roberts. Optimized synthesis of

RNA-protein fusions for *In Vitro* protein selection. *Methods Enzymol.*, 317:268–293, 2000.

[17] I. Rychlík, S. Chládek, and J. Žemlička. Release of peptide chains from the polylysyl-tRNA ribosome complex. *Biochim. Biophys. Acta*, 138:640–642, 1967.

[18] A. Bhuta, K. Quiggle, T. Ott, D. Ringer, and S. Chládek. Stereochemical control of ribosomal peptidyltransferase reaction. Role of amino acid side-chain orientation of acceptor substrate. *Biochemistry*, 20:8–15, 1981.

[19] H. Schagger and G.V. von Jagow. Tricine-sodium dodecyl sulfate-polyacrylamide gel electrophoresis for the separation of proteins in the range from 1 to 100 kDa. *Anal. Biochem.*, 166:368–379, 1987.

[20] EJ. Hengesh and AJ. Morris. Inhibition of peptide bond formation by cytidyl derivatives of puromycin. *Biochim. Biophys. Acta*, 299:654–661, 1973.

[21] DM. Graifer, OS. Fedorova, and GG. Karpova. Interaction of puromycin with acceptor site of human placenta 80 S ribosomes. *FEBS Lett.*, 277:4–6, 1990.

[22] J.R. Lorsch and D. Herschlag. Kinetic dissection of fundamental processes of eukaryotic translation initiation *in vitro*. *EMBO*, 18:6705–6717, 1999.

[23] A. Fersht. *Enzyme Structure and Mechanism*. W. H. Freeman and Company, New York, 1985.

[24] IA. Nazarenko and OC. Uhlenbeck. Defining a smaller RNA substrate for elongation factor Tu. *Biochemistry*, 34:2545–2552, 1995.

[25] N.Y. Sardesai, R. Green, and P. Schimmel. Efficient 50S ribosome-catalyzed peptide bond synthesis with an aminoacyl minihelix. *Biochemistry*, 38:12080–12088, 1999.

[26] J. Ellman, D. Mendel, S. Anthony-Cahill, CJ. Noren, and PG. Schultz. Biosynthetic method for introducing unnatural amino acids site-specifically into proteins. *Methods Enzymol.*, 202:301–336, 1991.

[27] DA. Dougherty. Unnatural amino acids as probes of protein structure and function. *Curr Opin Chem Biol*, 4:645–652, 2000.

[28] E. Baksht, N. de Groot, M. Sprinzl, and F. Cramer. Properties of tRNA species modified in the 3'-terminal ribose moiety in an eukaryotic ribosomal system. *Biochemistry*, 15:3639–3646, 1976.

[29] TW. Dreher, OC. Uhlenbeck, and KS. Browning. Quantitative assessment of EF-1α·GTP binding to aminoacyl-tRNAs, aminoacyl-viral RNA, and tRNA shows close correspondence to the RNA binding properties of EF-Tu. *J. Biol. Chem.*, 274:666–672, 1999.

[30] A. Varshavsky. The N-end rule: Functions, mysteries, uses. *Proc. Natl. Acad. Sci. U.S.A.*, 93:12142–12149, 1996.

[31] S.L. Wolin and P. Walter. Ribosome pausing and stacking during translation of a eukaryotic mRNA. *EMBO*, 7:3559–3569, 1988.

[32] J.N. Porter, R.I. Hewitt, C.W. Hesseltine, G. Krupka, J.A. Lowery, W.S. Wallace, N. Bohonos, and J.H. Williams. Achromycin: A new antibiotic having trypanocidal properties. *Antibiotics and Chemo.*, 11:409–410, 1952.

[33] J.A. Pérez-González, J. Vara, and A. Jiménez. Acetylation of puromycin by *Streptomyces alboniger* the producing organism. *Biochem. Biophys. Res. Commun.*, 113:772–777, 1983.

[34] P. Bhuta, G. Kumar, and S. Chládek. The peptidyltransferase center of *Escherichia coli* ribosomes: binding sites for the cytidine 3'-phosphate residues of

the aminoacyl-tRNA 3'- terminus and the interrelationships between the acceptor and donor sites. *Biochim. Biophys. Acta*, 696:208–211, 1982.

[35] J.L. Lessard and S. Pestka. Studies on the formation of transfer ribonucleic acid-ribosome complexes. xxiii. chloramphenicol, aminoacyl-oligonucleotides, and *Escherichia coli* ribosomes. *J. Biol. Chem.*, 247:6909–6912, 1972.

[36] N. Usman, K.K. Ogilvie, J.-Y. Jiang, and R.J. Cedergren. The automated chemical synthesis of long oligoribonucleotides using 2'-*O*-silylated ribonucleoside 3'-*O*-phosphoramidites on a controlled-pore glass support: Synthesis of a 43-nucleotide sequence similar to the 3'-half molecule of an *Escherichia coli* formylmethionine tRNA. *J. Am. Chem. Soc.*, 109:7845–7854, 1987.

[37] F. Wincott, A. DiRenzo, C. Shaffer, S. Grimm, D. Tracz, C. Workman, D. Sweedler, C. Gonzalez, S. Scaringe, and N. Usman. Synthesis, deprotection, analysis and purification of RNA and ribozymes. *Nucleic Acids Res.*, 23:2677–2684, 1995.